März 1970

KFK 1194

Institut für Angewandte Kernphysik

Band Mixing in ^{167}Er

W. Michaelis, F. Weller, U. Fanger, R. Gaeta, G. Markus,
H. Ottmar, H. Schmidt

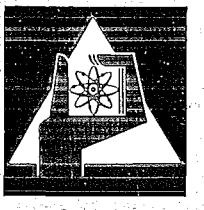

GESELLSCHAFT FÜR KERNFORSCHUNG M. B. H.
KARLSRUHE

1.E.1:
3.A

Nuclear Physics **A143** (1970) 225—254; © *North-Holland Publishing Co., Amsterdam*

BAND MIXING IN ^{167}Er

W. MICHAELIS, F. WELLER, U. FANGER, R. GAETA †, G. MARKUS ††,
H. OTTMAR and H. SCHMIDT

Institut für Angewandte Kernphysik, Kernforschungszentrum Karlsruhe,
Karlsruhe, Germany

Received 14 November 1969

Abstract: The level structure of ^{167}Er and the de-excitation mechanism in this nucleus have been studied by radiative capture of thermal neutrons in ^{166}Er. High-resolution measurements of the gamma-ray spectrum have been performed using a Ge(Li) anti-Compton spectrometer in the low-energy region and a Ge(Li) pair spectrometer for the high-energy transitions. Coincidence relationships have been obtained from measurements with a Ge(Li)-NaI(Tl) coincidence apparatus. The target was Er_2O_3 enriched to 95.6 % in ^{166}Er thus corresponding to a cross-section contribution of $(68.8^{+5.0}_{-6.4})$ % for ^{166}Er. More than 350 gamma-ray lines have been detected in the spectrum. Isotope assignment has been achieved by comparison of the spectra with those obtained from a sample of natural erbium. The high accuracy of the data and the coincidence results allow the construction of a transition diagram up to 1.5 MeV excitation energy. A large number of the observed energy levels have been assigned to specific configurations and their superimposed rotational bands. Detailed analysis of the data suggests considerable mixing between Nilsson states and the quadrupole vibrations Q_{22}, Q_{2-2} and Q_{20}. Theoretical calculations have been performed which take into account pair correlations, quasiparticle-phonon interaction, rotation-vibration interaction and Coriolis coupling. It is shown that neglect of pair correlations leads to unreasonable matrix elements. While quasiparticle-phonon interaction and Coriolis coupling have decisive influence on the level structure and the de-excitation mechanism, the effects due to rotation-vibration interaction are in general small. The model predicts the energy and structure of individual levels, branching ratios for gamma-ray transitions, multipole mixtures and partial gamma-ray half-lives. In most cases, good agreement is achieved between the theoretical calculations and the experimental results. The neutron separation energy was found to be 6436.15±0.48 keV.

E NUCLEAR REACTIONS ^{166}Er(n,γ), E = th; measured E_γ, I_γ, $\gamma\gamma$-coin; deduced Q. ^{167}Er deduced levels, J, π. Enriched target, Ge(Li) detectors.

1. Introduction

With increasing quantity and detail of experimental data on nuclear excitations the simple picture that assumes pure nuclear states with neglect of configuration mixing leads to serious disagreement between theoretical predictions and empirical results. In order to arrive at a better understanding of the various phenomena,

† Visiting scientist from Junta de Energia Nuclear, Ciudad Universitaria, Madrid.
†† Present address: Bundesministerium für Wissenschaft und Bildung, Bonn.

systematic experimental and theoretical studies are required. The rapid development of experimental techniques in gamma-ray spectroscopy has made feasible detailed investigations of nuclear structure by means of the radiative neutron capture process. In a recent paper on thermal neutron capture in ^{168}Yb we have pointed out the occurrence of considerable band mixing effects in ^{169}Yb (ref. [1])). Similar results have also been published on ^{165}Dy (ref. [2])). The purpose of the present work is to describe experimental data obtained from the (n, γ) reaction for the isotonic nucleus ^{167}Er, to provide a brief summary of theoretical considerations on this nucleus within the framework of the unified model and to discuss some obvious consequences of band mixing on the de-excitation mechanism.

As yet no exhaustive investigation of the ^{167}Er neutron capture transition diagram has been performed. Most of the available data have come from studies with the Risø bent crystal spectrometer [3]) and with a Ge(Li) pulse-height spectrometer [4]). In the first study 47 lines of the low-energy spectrum were assigned to ^{167}Er and 24 transitions were fitted into a level scheme. The second work examined the high-energy spectrum above 4330 keV using a sample of very high enrichment (99.97 %). The most recent investigations of ^{167}Er levels by means of charged-particle reactions are those given in refs. [5,6]). The decay of ^{167}Ho (3 h) and ^{167}Tm (9.6 d) to ^{167}Er has recently been studied with Ge(Li) and scintillation counters both in single and coincidence mode [7]). As to the earlier works we refer to the literature cited in refs. [3-7]).

In spite of these various investigations the information on the ^{167}Er level structure in the energy range up to 1.5 MeV has remained incomplete. In particular, the data on the de-excitation mechanism at medium and higher energies were still limited. While in the decay studies preferably low-energy (^{167}Tm) or high-spin states (^{167}Ho) are populated, the (n, γ) reaction is especially convenient for investigating levels with low spin irrespective of their energy, since the capture state has spin and parity $\frac{1}{2}^+$. The application of a Ge(Li) detector in Compton suppression technique allows the extension of the bent crystal high-resolution studies to higher gamma-ray energies and the favourable response characteristics of such a device make reliable checks on the isotope assignment of the observed transitions much less tedious. Therefore, it was felt useful to reinvestigate thoroughly the reaction ^{166}Er(n, γ)^{167}Er.

Theoretically, several attempts have been made in the past to extend the Nilsson model for deformed odd-mass nuclei [8-10]). In particular, the studies which take into account quasiparticle-phonon interaction and pair correlations have brought about a considerable improvement of the theory [9,10]). For a comparison with experimental data it is desirable to include all possible interactions between the various modes of nuclear motion into such considerations. A model which has proved to be very successful in interpreting the experimental results has been described elsewhere [1,11]). In the present research the calculations are extended to the nucleus ^{167}Er. The model includes quasiparticle-phonon interaction, Coriolis coupling, rotation-vibration interaction and pairing correlations.

2. Experimental procedure

2.1. TARGET

The measurements on ^{167}Er have been performed with a sample of Er_2O_3 enriched to 95.6 % in ^{166}Er. In spite of this relatively high enrichment care had to be taken in the isotope assignment of the gamma-ray lines. Due to the unfavourable cross section, the capture contribution of ^{166}Er was only 68.8 %. The main interference resulted from the target nucleus ^{167}Er which contributed with 31.1 % to the total capture cross section. Neutron capture in other erbium isotopes was negligible. The abundances of the isotopes in the sample together with the cross sections are summarized in table 1. In order to obtain a reliable isotope assignment each run was repeated with a target of natural erbium. More than 350 gamma-ray lines have been observed from the enriched sample. Details on the reaction ^{167}Er(n, γ)^{168}Er are given elsewhere [13]).

TABLE 1

Isotopic composition of the ^{166}Er sample and relative cross-section contributions

Isotope	Atomic %	Capture cross section for thermal neutrons [a]) (b)	Relative cross-section contribution (%)
^{162}Er	< 0.01	2.0 ± 0.2	< 0.001
^{164}Er	0.06	1.65 ± 0.17	< 0.002
^{166}Er	95.6 ± 0.1	45 ± 9	$68.8\ ^{+5.0}_{-6.4}$
^{167}Er	2.99 ± 0.05	650 ± 30	$31.1\ ^{+6.4}_{-5.0}$
^{168}Er	1.07 ± 0.05	2.03 ± 0.41	$0.035^{+0.017}_{-0.013}$
^{170}Er	0.24 ± 0.02	9 ± 2	$0.035^{+0.019}_{-0.015}$

[a]) Ref. [12]).

The data were also examined carefully for the possibility of contributions from likely chemical contaminants and, in fact, several lines were identified as arising from Sm and Gd isotopes.

2.2. SPECTROMETERS AND DATA PROCESSING

High-resolution measurements of the neutron capture gamma-ray spectrum have been performed using a Ge(Li) anti-Compton spectrometer [14–16]) in the energy range 125 to 1710 keV and a Ge(Li) five-detector pair spectrometer [2]) for transitions with energies above 2480 keV. Coincidence relationships have been studied by means of a Ge(Li)-NaI(Tl) coincidence system [17]) coupled to an on-line computer [18]). The data reported here were taken in 1967.

The anti-Compton spectrometer consisted of a 5 cm^3 Ge(Li) diode, a 50 cm ⌀ × 40 cm plastic scintillator of type NE 102 A and a 10.16 ⌀ × 15.24 cm NaI(Tl) detector placed at Compton scattering angles around 0°. For the 662 keV ^{137}Cs gamma ray the peak-to-Compton ratio was 73 : 1. The ratio photopeak height to Compton

minimum was about 150 : 1. Compton events from high-energy gamma rays were suppressed with high efficiency by the NaI(Tl) counter and by pulse-shape discrimination applied to the germanium detector signals. The energy resolution was 1.62 keV FWHM including long-term instabilities. Spectra were analysed using modified Gaussian functions which take into account the low-energy tail of the photopeaks. The energy calibration is based on the following standards:

^{57}Co	136.48 ±0.08 keV (ref. [19])),
^{192}Ir	295.938±0.009 keV (ref. [20])),
	316.486±0.010 keV (ref. [20])),
^{137}Cs	661.595±0.076 keV (ref. [21])),
^{60}Co	1173.226±0.040 keV (ref. [20])),
	1332.483±0.046 keV (ref. [20])),
^{88}Y	898.01 ±0.07 keV (ref. [21])),
	1836.08 ±0.07 keV (ref. [21])),
H(n, γ)	2223.29 ±0.07 keV (ref. [22])).

All spectra were carefully corrected for non-linearities in the amplifier chain and the ADC. Additional calibration points were obtained by means of a ultra-high precision pulser. The procedures applied in spectrum stabilization, spectrum analysis, calibration and non-linearity correction are described in detail in ref. [16]). The response function of the spectrometer was experimentally determined with a set of absolutely calibrated gamma-ray sources (^{57}Co±2 %; ^{203}Hg±1 %; ^{22}Na±1 %; ^{137}Cs±2 %; ^{54}Mn±1 %; ^{60}Co±1 % and ^{88}Y±2 %).

The five-crystal pair spectrometer consisted of a planar germanium diode and four bevelled 7.62 cm ⌀ × 7.62 cm NaI(Tl) secondary detectors. A coarse investigation of the total spectrum above 2480 keV was performed using a diode with 2.7 cm^2 × 0.2 cm sensitive volume. In a second run the spectrum between 4330 and 6230 keV was studied in more detail. A Ge(Li) counter with 7 cm^2 × 0.7 cm volume was used in this measurement. The energy resolution was 8.3 keV FWHM at 6000 keV gamma-ray energy. The calibration is based on the following standards:

^{14}N(n, γ)	4508.8±0.3 keV	(ref. [23])).
	5268.5±0.2 keV	
	5297.4±0.3 keV	
	5533.0±0.3 keV	
	5562.0±0.3 keV	
	6322.1±0.4 keV	

The procedures in spectrum stabilization and analysis, in calibration and non-linearity correction were similar to those applied in the low-energy region. For the second run the response function was determined using the well-known intensities [24])

from the reaction ^{14}N(n, γ)^{15}N. Gamma-ray intensities below 4330 keV are based on the results of Monte Carlo calculations for the double-escape peak efficiency of planar Ge(Li) diodes [25]). The uncertainties inherent in this procedure introduced relatively high errors in the intensities below 4330 keV.

The coincidence spectrometer consisted of a 34 cm^3 coaxially drifted germanium counter and a 7.62 cm ⌀ × 7.62 cm NaI(Tl) detector. A brief discussion of the technique used for analysing complex coincidence spectra by means of an on-line computer may be found in ref. [17]).

2.3. NEUTRON BEAMS

The anti-Compton spectrometer and the pair spectrometer were located at the two exits of a tangential beam hole which passes through the heavy water reflector of the reactor FR2. The external targets were irradiated only by neutrons emerging from a 75 mm long 50 mm ⌀ graphite scatterer placed in the centre of the channel. Bismuth single crystal filters of 20 cm length reduced the fast neutron and gamma contamination in the beams. For the coincidence measurements thermal neutrons from a radial reflector channel were diffracted from the (111) planes of a 4 cm thick lead single crystal at a Bragg angle of 12.2°. Details on the geometric arrangements and the properties of the neutron beams may be found in refs.[1,2]) and the literature cited there.

3. Experimental results

3.1. NEUTRON CAPTURE GAMMA-RAY SPECTRUM IN THE ENERGY RANGE 125 TO 1710 keV

Gamma-ray energies and intensities as observed with the anti-Compton spectrometer from the enriched sample are summarized in table 2. Due to the complex structure of the spectrum, part of the lines may represent closely spaced doublets or triplets. If a peak which is now assumed to correspond to a single gamma ray turns out to be a multiplet, the energy given in the table refers to the centroid and the intensity is the total intensity of the components. For determining the quoted uncertainties in the energy values consideration was given to: (i) the statistical fluctuations in the spectrum, (ii) the goodness of fit obtained in the spectrum analysis, (iii) possible errors in the non-linearity correction function and (iv) the uncertainties associated with the energy standards.

The gamma-ray intensities listed in table 2 are relative intensities. They were normalized to a value of 6.8 for the 531.54 keV line. This value was adopted from ref. [3]). As stated by the author the deviation from the absolute intensity in photons per 100 captures is not more than about 30 %. The errors quoted for the intensities in table 2 include uncertainties arising from the statistics, the fitting procedure and the spectrometer response function.

In order to facilitate the survey of the data, the last column in table 2 gives the assignment of the lines in the gamma-ray transition diagram (see sect. 4).

TABLE 2

Neutron capture gamma rays in the energy range from 125 to 1710 keV

E_γ (keV)	$\pm\Delta E_\gamma$ (eV)	I_γ	$\pm\Delta I_\gamma$	Assignment [a]) remarks
131.70	250	0.3 [b])	0.1	413 → 282
148.43	200	0.3 [b])	0.1	413 → 265
160.4	500	<0.2 [b])		442 → 282
162.9	600	<0.1 [b])		
167.4	500	<0.1 [b])		
174.0	500	<0.1 [b])		
177.65	450	<0.1 [b])		178 → 0
184.31	60	11.0 [b])	2.0	168
193.5	500	<0.1 [b])		
198.30	70	6.3 [b])	1.5	168
207.84	80	10.0	2.0	208 → 0
217.51	100	0.53	0.10	168
221.9	500	0.05	0.01	168
226.9	600	<0.03		
231.9	600	<0.03		168
237.78	120	0.13	0.02	668 → 430
249.8	600	<0.03		
255.81	150	0.19	0.04	168
269.23	300	0.10	0.02	168
274.4	800	0.10	0.03	167; small 168
277.8	900	0.09	0.02	167
284.68	80	3.85	0.76	168
294.0	700	<0.03		168
308.7	600	<0.03		decay 171
315.57	200	0.085	0.017	746 → 430; ≈ 50 % 168
317.4	800	<0.04		u
321.35	100	0.71	0.11	668 → 347
333.93	80	2.5	0.4	^{150}Sm
337.88	450	0.05	0.02	u
346.50	70	4.90	0.75	347 → 0
350.84	250	0.14	0.03	167; impurities contribute
357.4	750	<0.03		u
365.8	500	<0.03		u
371.35	180	0.135	0.028	168+167
379.84	200	0.146	0.030	168; d
382.95	480	0.046	0.010	168
386.33	250	0.087	0.018	668 → 282
396.46	150	0.245	0.040	168
398.90	160	0.21	0.02	746 → 347
403.20	150	0.186	0.025	668 → 265; ≈ 20 % ^{150}Sm
406.68	280	0.08	0.02	167; ≈ 25 % ^{150}Sm
416.99	180	0.42	0.06	d; 763 → 347; ≈ 15 % 168
422.34	100	0.49	0.05	168
426.28	220	0.143	0.020	1179 → 753
430.00	280	0.137	0.020	d; 430 → 0; ≈ 80 % 168
439.43	80	1.69	0.17	^{150}Sm
444.0	300	0.152	0.022	1254 → 753
447.45	100	1.03	0.11	168
453.4	1000	0.06	0.02	167(?)

TABLE 2
(continued)

E_γ (keV)	$\pm\Delta E_\gamma$ (eV)	I_γ	$\pm\Delta I_\gamma$	Assignment [a]) remarks
455.32	250	0.205	0.045	d; 802 → 347; ≈ 25 % 168
457.74	250	0.22	0.03	168
460.5	800	0.05	0.03	668 → 208
462.62	400	0.14	0.03	d; 745 → 282; ≈ 40 % 168
471.10 [c])	400	0.15 [c])	0.08	753 → 282
474.45 [c])	400	0.2 [c])	0.1	at least predominantly 168
480.1 [c])	800	<0.1 [c])		at least predominantly 168
487.93	120	0.88	0.05	753 → 265
494.37	90	1.13	0.06	574 → 79
498.57	90	1.48	0.08	763 → 265; <10 % 168
505.65	180	0.35	0.04	^{150}Sm
511.17	300			complex
515.8	600	0.13	0.06	168; pd
520.6	500	0.33	0.08	d; 802 → 282; ≈ 30 % 168
527.89	280	0.22	0.10	168
531.54	80	6.8		532 → 0; intensity normalization
533.8	500	<0.2		168
543.95	300	0.90	0.30	168
545.34	450	1.14	0.29	753 → 208
547.45	350	0.60	0.12	168
554.8	500	0.44	0.07	1086 → 532; see text
557.1	900	0.09	0.04	168
559.81	320	1.38	0.13	168
569.11	300	0.55	0.05	168
573.78	90	2.80	0.23	574 → 0
578.7	500	<0.2		u; 167(?)
580.23	250	0.25	0.08	168
583.79	300	0.38	0.15	167+168
584.30	450	0.33	0.13	168+^{150}Sm
591.82	150	0.87	0.09	592 → 0
593.88	120	1.55	0.15	802 → 208
601.80	350	0.29	0.06	168
603.85	250	0.73	0.07	1135 → 532; see text
613.53	280	0.275	0.040	predominantly 167
617.14	280	0.315	0.035	predominantly 167
620.47	320	0.19	0.05	168
631.76	80	3.03	0.27	168
639.32	180	0.45	0.05	168+≈ 25 % 167
645.74	150	0.97	0.09	d; 1059 → 413, ≈ 40 % 168 see text
650.0	500	0.10	0.04	167(?)
656.9	600	0.06	0.03	u
661.18	320	0.17	0.04	167
668.3	700	0.06	0.03	pd; 668 → 0, 168(?)
674.25	220	0.31	0.04	pd; 168+^{150}Sm
679.2	800	0.135	0.027	168
687.48	400	0.07	0.02	168
691.80	220	0.33	0.05	pd; 167+168

TABLE 2
(continued)

E_γ (keV)	$\pm\Delta E_\gamma$ (eV)	I_γ	$\pm\Delta I_\gamma$	Assignment [a]) remarks
694.9	500	0.07	0.02	167
700.6	600	0.04	0.02	168
703.5	500	0.10	0.03	168
712.59	250	0.46	0.09	168 + ^{150}Sm
715.29	200	0.91	0.13	168
719.98	180	1.16	0.12	168
723.4	900	0.17	0.07	168
730.69	80	4.98	0.50	168
737.62	200	0.83	0.09	d; 168 + ^{150}Sm
741.37	90	2.85	0.25	168
748.24	180	0.71	0.07	168
756.3	1000	0.08	0.03	u
761.9	1000	0.07	0.03	u
767.9	1000	0.05	0.03	u
777.0	700	0.11	0.04	1059 → 292
779.9	500	0.16	0.04	168
789.83	280	0.25	0.05	168
794.00	250	0.28	0.04	1059 → 265
798.98	220	0.88	0.09	168
810.53	120	2.42	0.24	167; see text
815.97	80	18.6	1.7	168
821.04	120	2.98	0.30	168
823.93	450	0.74	0.15	168
829.94	180	1.97	0.30	168
832.2	650	0.44	0.17	168
840.8	500	0.27	0.08	1254 → 413; small contribution 168
845.2	900	0.10	0.05	u
853.40	90	3.54	0.36	168
862.39	200	0.79	0.08	168
870.5	500	0.17	0.04	1135 → 265
878.52	180	0.46	0.06	1086 → 208
884.45	280	0.24	0.05	168
898.52	150	0.68	0.08	167; ≈ 50 % 168
909.37	420	0.16	0.03	1662 → 753
914.94	80	3.25	0.40	168
924.56	350	0.25	0.05	1206 → 282
928.83	180	0.76	0.09	168
932.26	350	0.36	0.07	168
940.8	500	0.13	0.03	1206 → 265
944.8	500	0.14	0.03	168
953.3	900	0.11	0.03	168
956.2	900	0.21	0.06	168
962.7	600	0.82	0.10	1227 → 265; ≈ 60 % 168
966.1	800	0.53	0.10	168
971.0	700	0.46	0.12	1179 → 208
977.7	800	0.24	0.10	168
981.0	800	0.17	0.07	168
989.1	1800	0.13	0.06	u; 1254 → 265

TABLE 2
(continued)

E_γ (keV)	$\pm\Delta E_\gamma$ (eV)	I_γ	$\pm\Delta I_\gamma$	Assignment [a]) remarks
995.2	600	0.16	0.06	167+168
999.62	250	0.48	0.09	168
1011.4	700	0.56	0.12	167
1012.5	800	0.44	0.18	168
1019.37	180	0.77	0.15	1227 → 208
1025.73	250	0.45	0.09	168
1030.1	700	0.15	0.05	167
1037.83	120	1.16	0.20	1384 → 347
1049.1	900	0.13	0.06	u
1058.51	300	0.33	0.07	167
1063.6	1000	0.09	0.04	pd; 168
1068.2	500	0.25	0.05	168
1088.9	1000	0.08	0.04	u
1095.1	1000	0.17	0.08	168(?)
1098.3	1000	0.13	0.06	168(?)
1106.7	500	0.32	0.06	168
1111.3	800	0.12	0.04	167
1143.0	1000	0.20	0.06	168
1146.68	250	0.62	0.12	pd; 167+168
1159.8	700	0.16	0.05	168
1167.80	200	0.83	0.16	168
1173.41	250	0.46	0.09	impurities contribute
1181.1	800	0.15	0.05	168
1196.5	500	0.24	0.06	168
1201.70	450	0.49	0.09	predominantly d.e. H(n, γ)
1212.98	450	0.24	0.05	168
1219.6	1500	0.07	0.03	u
1223.35	300	0.47	0.10	1755 → 532
1229.45	450	0.28	0.07	168
1235.2	500	0.20	0.07	168
1260.4	700	0.14	0.04	168
1264.7	1500	0.13	0.06	168
1273.0	500	0.65	0.13	pd; 167+168
1277.65	250	1.51	0.40	168
1280.5	500	0.42	0.13	1545 → 265
1294.5	500	0.42	0.11	1641 → 347
1298.0	600	0.44	0.11	167
1305.2	1200	0.12	0.05	167
1310.2	500	0.93	0.19	168
1324.0	500	0.95	0.20	168
1331.73	450	1.04	0.21	168
1341.5	500	0.48	0.10	167
1351.1	600	0.59	0.18	168
1353.5	600	0.82	0.22	167+168
1359.5	700	0.19	0.08	168
1366.7	800	0.14	0.06	168
1373.3	600	0.28	0.07	pd; 167+168
1381.5	500	0.80	0.16	167
1384.4	900	0.22	0.08	1649 → 265

TABLE 2
(continued)

E_γ (keV)	$\pm\Delta E_\gamma$ (eV)	I_γ	$\pm\Delta I_\gamma$	Assignments [a]) remarks
1392.6	500	0.43	0.09	168
1398.2	1200	<0.1		168
1409.5	1200	<0.15		168
1414.9	1200	<0.15		168
1432.9	800	0.18	0.07	167+168
1437.7	700	0.34	0.07	167
1441.5	600	0.51	0.10	1649 → 208; ≈ 25 % 168
1453.9	500	0.82	0.16	1662 → 208
1485.2	800	0.26	0.05	167+168
1491.7	1500	0.11	0.05	u
1503.0	1200	0.23	0.08	167
1507.1	1200	0.24	0.08	168
1516.3	800	0.31	0.08	168
1523.8	700	0.37	0.09	167; small 168
1534.4	2500	0.10	0.05	u
1538.0	2000	0.10	0.05	u
1554.1	2500	0.11	0.05	u
1556.9	1500	0.25	0.09	167+168
1560.9	1800	0.13	0.06	168
1571.2	1200	0.16	0.07	168
1581.1	900	0.28	0.08	168
1650.2	800	0.42	0.13	168
1672.9	900	0.19	0.08	168
1708.5	800	0.32	0.09	167

Target: Er_2O_3 enriched to 95.6 % in ^{166}Er. The intensities are normalized to a value of 6.8 for the 531.54 keV gamma ray (see text).

[a]) If a gamma ray is assigned to a transition between levels with energies E_1 and E_2 in ^{167}Er, this is indicated by $E_1 \rightarrow E_2$. Gamma lines which are attributed to ^{167}Er, but were not fitted into the transition diagram are labelled with the mass number 167. The mass number 168 marks transitions which are assigned to ^{168}Er. The following abbreviations are used: u = uncertain line, pd = possible doublet, d = doublet.

[b]) Below 200 keV the pulse-shape discrimination affects the intensity determination.

[c]) Energy and intensity determination are affected by background from the reaction $^{10}B(n, \alpha)$.

A typical sectional display of the gamma-ray spectrum is represented in fig. 1. The example clearly demonstrates both the high resolution and the effective suppression of Compton events.

3.2. NEUTRON CAPTURE GAMMA-RAY SPECTRUM ABOVE 2480 keV

Table 3 summarizes the gamma-ray energies and intensities as obtained with the pair spectrometer. The detailed analysis performed in the energy range from 4330 to 6230 keV revealed excellent agreement for the ^{167}Er lines with the data which have been reported in ref. [4]). The intensities quoted are relative values normalized to 100 for the 6171 keV gamma ray. In ref. [4]) an absolute value of 23 photons per

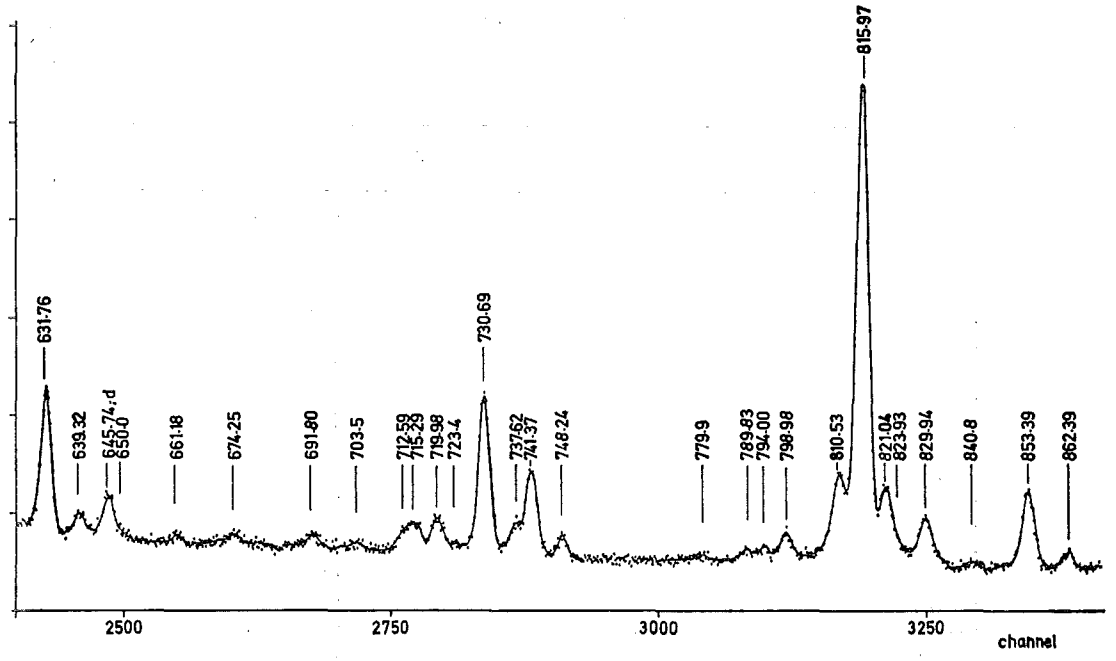

Fig. 1. Sectional display of the capture spectrum as observed with the anti-Compton spectrometer from the enriched sample.

TABLE 3

Neutron capture gamma rays above 2480 keV

E_γ (keV)	$\pm\Delta E_\gamma$ (keV)	I_γ	$\pm\Delta I_\gamma$	Assignment [a]) remarks [b])
6228.23	0.35	395	40	C → 208
6171.2	0.5	100		C → 265
6137.0	0.4	13	2	168
6051.5	0.5	10	2	168
5942.8	0.7	5	1	168
5904 [c])				C → 532
5877.6	0.4	18	3	168
5682.8	0.7	≈10		d; C → 753; 168
5670 [c])				C → 763
5634.2	0.7	<10		C → 802
5369.4	0.7	8	2	168
5359.6	0.9	16	3	168
5351.0	0.9	20	3	C → 1086; ≈ 15 % 168
5293.2	0.8	17	3	d; 168
5257.7	0.6	19	4	C → 1179
5242.1	0.7	5	2	168
5210.2	0.9	58	10	C → 1227; ≈ 15 % 168
5169.7	0.6	12	2	168
5139.5	1.2	1.6	0.8	168
5119.6	0.9	4.5	1.0	168
5112.4	0.7	10	2	168
5097.5	1.3	1.5	0.7	168
5071.2	0.7	5.0	1.5	168

TABLE 3
(continued)

E_γ (keV)	$\pm\Delta E_\gamma$ (keV)	I_γ	$\pm\Delta I_\gamma$	Assignment [a]) remarks [b])
5051.3	0.7	16	4	C → 1384
5034.3	1.1	6.5	2.0	168
5002.4	0.9	5.0	1.5	168
4993.7	1.5	2	1	u; 168
4983.8	0.8	5.0	1.5	168
4959.0	1.4	1.8	0.9	168
4945.9	0.8	5.3	1.5	168
4921.8	0.5	16.5	3.5	168
4896.0	1.5	4.6	1.5	168
4891 [c])				C → 1545
4877.3	1.5	1.5	0.7	168
4871.0	1.5	7	1	C → 1565
4853.5	2.0	2	1	168
4801.0	0.6	7.3	1.5	168
4792.8	2.0	6	2	C → 1641
4787.0	1.5	17	3	C → 1649
4775.3	0.9	25	5	C → 1662
4744.9	1.0	6.1	1.5	168
4716.6	0.9	28	5	C → 1719
4682.0	0.9	18	4	C → 1755
4671.0	1.3	3.0	1.0	168
4659.1	1.4	2.2	0.7	168
4644.0	1.0	7	2	C → 1792; ≈ 60 % 168
4625.9	1.2	7	2	C → 1810; ≈ 25 % 168
4614.0	1.1	2.7	0.9	168
4597.9	2.5	1.0	0.5	u; 168
4576.3	1.0	3.8	0.9	168
4567.3	1.0	8	2	C → 1869
4538.9	1.1	2.8	0.6	168
4510.2	1.5	3.7	0.8	168
4513 [c])				C → 1923
4498.9	1.8	5.0	1.0	168
4486.7	1.1	17	4	C → 1950; partially 168
4445.4	0.8	5.6	1.2	168
4390.9	0.8	8.6	1.8	168
4372.0	1.5	10	2	C → 2065
4358	6	<5		168
4341	5	<8		C → 2095
4331	5	10	3	C → 2105
4326	6	79		Note: Second group of transitions; no particular effort made after this point to separate the 167 intensity from other Er isotopes
4285	8	<35		
4270	5	65		
4247	8	<42		
4229	7	<35		
4176	7	53		
4160	5	100		
4129	6	68		
4112	5	79		
4075	6	53		

TABLE 3
(continued)

E_γ (keV)	$\pm\Delta E_\gamma$ (keV)	I_γ	$\pm\Delta I_\gamma$	Assignment [a]) remarks [b])
4054	7	47		d
4040	8	<35		
4013	7	50		d
4002	7	<35		
3990	5	58		
3980	7	<35		u
3973	5	39		
3956	6	<35		
3942	7	<35		u
3922	6	45		
3915	5	55		
3891	4	58		
3874	6	42		d
3851	5	79		pd
3822	6	44		pd
3804	5	62		
3788	6	39		
3782	5	55		
3771	6	50		
3757	4	94		
3743	7	<35		u
3717	4	65		
3696	4	76		
3685	5	50		
3675	7	<35		
3655	5	55		
3641	7	<28		
3625	7	<28		u
3616	5	62		
3584	4	68		
3574	7	<35		
3541	4	100		Note: Third group of transitions
3518	4	83		
3494	6	41		d
3466	5	64		
3452	6	56		
3443	6	41		
3429	4	79		
3399	4	76		
3364	5	31		
3354	5	36		
3343	4	41		
3320	4	52		
3309	5	35		
3295	5	38		
3263	5	38		
3249	5	48		
3240	5	64		d
3225	7	28		

TABLE 3
(continued)

E_γ (keV)	$\pm\Delta E_\gamma$ (keV)	I_γ	$\pm\Delta I_\gamma$	Assignment [a]) remarks [b])
3210	7	34		
3202	5	39		
3194	6			
3173	6			
3162	4			
3140	4			
3116	7			
3099	4			
3091	6			
3076	4			
3058	7			
3043	5			pd
3033	5			
2988	6			d
2972	5			
2954	6			
2943	4			
2923	6			
2907	6			
2891	4			
2870	6			d
2854	5			
2830	5			
2812	5			
2800	6			u
2786	6			
2766	7			
2753	7			u
2736	7			
2728	5			
2705	6			
2696	5			
2674	7			
2660	6			
2648	6			
2620	6			pd
2597	6			
2574	6			
2554	8			d
2532	8			
2520	8			
2506	8			u
2481	8			

Target: Er_2O_3 enriched to 95.6 %. The intensities are relative values. They are normalized within three subgroups to a value of 100 for the gamma rays at 6172.2, 4160 and 3541 keV.

[a]) C → E_a denotes primary transition from compound state in ^{167}Er to level with excitation energy E_a; 168 marks transitions assigned to ^{168}Er.

[b]) d = doublet, pd = possible doublet, u = uncertain line.

[c]) Gamma rays not established with confidence; energy values adopted from ref. [4]).

1000 captures has been assigned to this transition. The above remarks (subsect. 3.1.) on the evaluation of the errors and the possible occurrence of unresolved complex structures also apply to the energy interval discussed here. Four weak gamma-ray lines (at 5904, 5670, 4891 and 4531 keV) which have been observed in ref. [4]) could not be established with confidence due to the still insufficient enrichment of the target. At least two of these lines (at 5904 and 5670 keV), however, are well consistent with the level scheme derived from the present research (cf. fig. 2) and their existence is confirmed by the coincidence measurements described in subsect. 3.3.

In the energy range from 2480 to 4330 keV no particular effort was made to separate the ^{167}Er intensities from other isotopes. Since the intensities are based on theoretical response functions, they were normalized to 100 for an intense line within each of two subgroups.

3.3. COINCIDENCE MEASUREMENTS

High-resolution coincidence spectra covering the low-energy region were obtained with the germanium detector by setting digital windows in the high-energy spectrum of the NaI counter. The precise knowledge of the singles spectra was of considerable aid in selecting optimum window widths and positions and in interpreting the results. The spectra suggest the following coincidence relationships: 5210–1019 keV, (5210–963 keV), 5258–971 keV, 5634–594 keV, 5634–455 keV, 5670–499 keV, 5670–417 keV, 5683–545 keV, 5683–488 keV, 5683–471 keV and 5904–532 keV.

4. Transition diagram of ^{167}Er

The present research suggests a considerably extended transition diagram as represented in fig. 2. The arrow widths give an approximate indication of the gamma-ray intensities. Most of the lines were fitted into the diagram using the Ritz combination principle. Transitions marked with the letter "c" have been clearly observed in coincidence measurements and their position in the decay scheme is well established. Dashed arrows mean that the available data suggest the existence of these gamma rays and the position shown, but the assignment is considered to be somewhat tentative. Transitions labelled with an asterisk have been adopted from previous investigations provided that the assignment is consistent with the present study. For the sake of completeness the results obtained from charged-particle reactions have also been included in the decay scheme. Levels labelled with the letter "a" have been observed in (d, p) reactions [5]). Letter "b" indicates excited states detected in inelastic scattering of deuterons [6]). If a gamma-ray transition with energy below 350 keV has also been reported from crystal diffraction measurements [3]), the energy value was taken from the previous data because of the higher accuracy in this energy region.

Several missing gamma rays which are expected on the basis of the proposed decay scheme could not be identified with confidence since they are obscured by strong transitions arising from ^{168}Er or chemical contaminants in the sample.

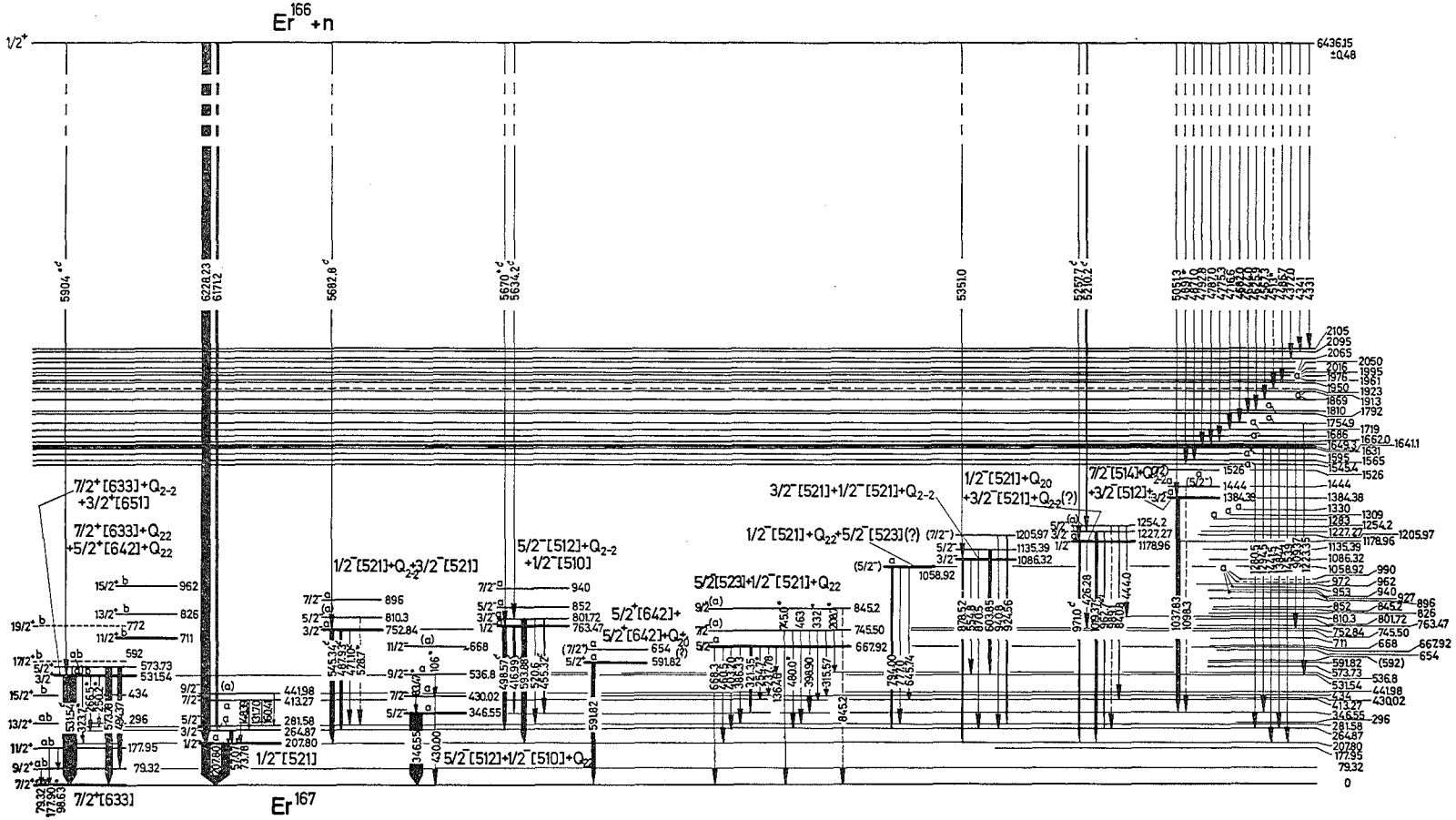

Fig. 2. Transition diagram of ^{167}Er. See comments in the text.

For instance, the level at 852 keV should be de-excited by gamma rays with energy 439 and 570 keV which proceed to the levels at 413 and 282 keV. This follows from the systematics when looking at the data which we have obtained for the isotonic nucleus [1]) ^{169}Yb. Both transitions coincide in energy with strong lines from ^{150}Sm and ^{168}Er. Possible transitions de-exciting the same level to the states at 347 and 430 keV are obscured in a similar manner. Other examples are the gamma rays at 821, 851 and 914 keV which are expected to proceed from the levels at 1086, 1059 and 1179 keV. The gamma line observed at 545 keV is most probably a doublet with a very small energy spacing. The second component is believed to de-excite the 810 keV state (see also ^{169}Yb in ref. [1])).

The spectroscopic interpretation given in the transition diagram is based on a detailed analysis of the experimental data and on the theoretical considerations described in the subsequent sections of this report. Only the dominant components of the structure have been included in fig. 2. For details we refer to table 6 in sect. 5. As is to be expected from the results for the isotonic species ^{165}Dy and ^{169}Yb, considerable band mixing is also observed in ^{167}Er. While for the positive parity states both Coriolis coupling and quasiparticle-phonon interaction exhibit important influence, the properties of the negative parity states are mainly determined by quasiparticle-phonon interaction. The effects due to rotation-vibration interaction are in general small. Experimentally, evidence for the presence of configuration mixing can be deduced primarily from the partial gamma-ray half-lives, the branching ratios to different rotational bands and the excitation energies. This will be discussed in more detail in sect. 6. A very obvious example for strong band mixing is provided by the anomalous de-excitation of the gamma-vibrational band at 763 keV.

Some levels in fig. 2 require special comments. Investigation of the (d, p) reaction[5]) revealed two relatively weak states at 595 and 654 keV which remained unassigned. In this excitation region the Nilsson orbital $\frac{5}{2}^+[642]$ is expected (cf. table 6). From the view of the theoretical differential (d, p) cross sections for this state there is a possibility that one of the observed levels is the $\frac{9}{2}^+$ member of the $\frac{5}{2}^+[642]$ orbital. Only minute intensities are predicted for the other members of this band. On the other hand, the $\frac{5}{2}^+$ level should be populated in the (n, γ) reaction with marked intensity. De-excitation is expected to occur preferably to the ground state by M1 radiation. The only gamma ray which has reasonable intensity and energy and which is not placed elsewhere in the decay scheme is that at 592 keV. This line was not detected in coincidence with primary transitions above 5000 keV and, in fact, the $\frac{5}{2}^+$ level should not be populated directly from the capture state with measurable intensity. In ^{169}Yb the (d, p) and (d, t) reactions [26]) revealed a rotational band at 584 keV which has tentatively been assigned as the orbital $\frac{5}{2}^+[642]$. In the (n, γ) reaction on this nucleus [1]) a very strong transition was observed with an energy of 591 keV. For intensity reasons it is likely that this gamma ray corresponds to a ground state transition. In ref. [27]) the multipole character was found to be M1 and the $\frac{5}{2}^+[642]$ state was placed at 590 keV. Thus there is some evidence that in ^{167}Er the $\frac{5}{2}^+[642]$

orbital occurs at 592 keV. However, due to the apparent inconsistency with the (d, p) data this assignment has to be considered to be somewhat tentative. The difficulties in arriving at definite conclusions are perhaps not too surprising, since one expects considerable confusion to arise for the positive parity states from strong Coriolis coupling. In addition the possibility of unidentified impurities in the two positions of the relevant proton groups cannot be ruled out.

The rotational bands at 1059, 1086, 1179 and 1384 keV occur at excitation energies, where the mixing of states prohibits confident use of "fingerprint" patterns in the (d, p) reaction. A very weak proton group has been observed in ref. [5]) at 1056 keV. Three gamma-ray lines can be fitted between a level at 1059 keV and the $\frac{3}{2}^-$, $\frac{5}{2}^-$ and $\frac{7}{2}^-$ members of the $\frac{1}{2}^-[521]$ rotational band. One expects in this region the γ-vibration $\frac{1}{2}^-[521]+Q_{22}$ (cf. subsect. 6.1). The failure to observe primary feeding from the capture state and the branching ratio of the transitions at 777 and 794 keV are consistent with this assignment. Unfortunately, the transition to the state $\frac{1}{2}^-\ \frac{1}{2}[521]$ is obscured. The 646 keV gamma ray is much stronger than predicted theoretically. If the assignment $\frac{1}{2}^-[521]+Q_{22}$ is correct, it is therefore probable that only part of the intensity belongs to the transition leaving the level at 1059 keV.

The occurrence of a primary transition at 5351 keV with likely E1 character and the low-energy data from table 2 suggest a $\frac{3}{2}^-$ rotational band at 1086 keV that may be interpreted as the configuration $\frac{3}{2}^-[521]+\frac{1}{2}^-[521]+Q_{2-2}$. Into this band two gamma rays (at 555 and 604 keV) can be fitted which should have E1 multipolarity, if their position in the decay scheme is correct. The intensity of both transitions is much higher than predicted by theory. Intensity considerations therefore throw some doubt on the position shown in fig. 2. On the other hand, the calculations for E1 transition probabilities are very sensitive to the parameters used and the results may be wrong by several orders of magnitude. In addition, the model described here does not include admixtures of octupole vibrations which might change the calculated E1 transition probabilities considerably.

The high-energy doublet observed at 5210 and 5258 keV and the de-excitation data which can be derived from the low-energy singles spectra and the coincidence measurements give ample evidence for the occurrence of a $K = \frac{1}{2}^-$ band at 1179 keV with rotational members at 1227 and 1254 keV. The characteristic energy pattern of these levels suggests that the origin of this band is the $K = 0$ β-vibration coupled to the $\frac{1}{2}^-[521]$ particle state. Such a band is expected to have inertial and decoupling parameters similar in value to those for the particle configuration (cf. table 6). The only alternative $K = \frac{1}{2}^-$ state predicted in this energy region has the dominant structure $\frac{5}{2}^-[523]+Q_{2-2}$. This rotational band, however, should exhibit a quite different de-excitation mechanism and the decoupling parameter is expected to be small.

The intensity of the 5051 keV primary transition is consistent with the assumption of electric dipole character for this gamma ray. The spin of the 1384 keV state is therefore $\frac{1}{2}^-$ or $\frac{3}{2}^-$. Since no other radiation from the capture state is observed within a reasonable energy interval around 5051 keV, the spin $\frac{3}{2}^-$ seems to be more probable.

In addition, two levels at 1444 and 1526 keV which are populated in the (d, p) reaction have appropriate energy spacings to fit into a $K = \frac{3}{2}$ rotational band. Only one strong transition de-exciting the 1384 keV state can be placed with confidence into the level scheme. This transition proceeds to the orbital $\frac{5}{2}^-[512]$. The multipolarity should then be M1 which is consistent with the observed intensity. A possible interpretation for the 1384 keV band is that it corresponds to the configuration $\frac{7}{2}^-[514]+Q_{2-2}+\frac{3}{2}^-[512]+\ldots$. The Nilsson states $\frac{7}{2}^-[514]$ and $\frac{3}{2}^-[512]$ are connected by a large E2 matrix element. Thus the $\frac{3}{2}^-[512]$ state is expected to be strongly admixed into the wave function of the gamma-vibrational band based on the state $\frac{7}{2}^-[514]$. This admixture may be responsible for the strong M1 transition to the orbital $\frac{5}{2}^-[512]$, since the corresponding M1 matrix element is large. The relative differential cross sections observed in the (d, p) reaction for the levels at 1384, 1444 and 1526 keV are not in contradiction to the presence of a $\frac{3}{2}^-[512]$ single-particle strength.

It is worth mentioning that in virtue of its energy the 810.53 keV gamma ray from table 2 can be fitted very well between the levels at 573.73 and 1384.38 keV. However, the high intensity seems to be inconsistent with this position in the decay scheme.

Below 1500 keV excitation energy all levels with probable spin values $\frac{1}{2}^-$ or $\frac{3}{2}^-$ are found to be populated directly from the capture state. A striking feature of the high-energy spectrum is the small radiation width for the E1 transitions to the levels at 763 and 802 keV and the remarkably high intensity of the 6228 keV gamma ray which feeds the state $\frac{1}{2}^-[521]$.

From the most intense primary transitions at 6228 and 6171 keV and the corresponding level energies we obtain the energy sums 6436.03 keV and 6436.07 keV. Including the recoil correction the neutron separation energy is calculated to be 6436.15 ± 0.48 keV. The result is in excellent agreement with the previously reported binding energy for the (n, γ) reaction [4]) of 6436 ± 3 keV and the (d, p) value of 6434 ± 10 keV. The separation energy 6444 ± 5 keV as derived from mass spectrometric data † is outside the experimental error of the present research.

5. Theoretical considerations

In order to arrive at a better understanding of the experimental data, calculations have been performed which take into account pair correlation, quasiparticle-phonon interaction, rotation-vibration interaction and Coriolis coupling. Since a solution with the exact Hamiltonian is beyond the possibilities of present theoretical nuclear physics, it is convenient to use a phenomenological approach. Such a procedure is justified, if only few additional parameters are introduced, if these parameters have a well defined physical meaning and if an extensive set of data is predicted which can be examined experimentally. The calculations that will be outlined here very briefly reveal the excitation energy and structure of individual levels, absolute transition rates and partial gamma-ray half-lives, multipolarity mixtures and branching ratios. Details of the model may be found in refs. [1,11]).

† Private communication cited in ref. [4]).

The Hamiltonian is written as [28,29])

$$H = H_0 + H',$$

with

$$H_0 = H_N + H_{0c}.$$

Here H_N is the Nilsson Hamiltonian [30]) and H_{0c} describes the undisturbed collective motion, i.e. the rotation of the nucleus and the β and γ vibrations. The interactions between the various modes of motion are taken into account by H'. This term includes the Coriolis coupling, the particle-phonon interaction and the rotation-vibration interaction.

TABLE 4

Single-particle levels and energies from the BCS-calculation for ^{167}Er

No.	$\Omega^\pi[Nn_z\Lambda]$	ε_ν $[\hbar\omega_0]$	E_ν $[\hbar\omega_0]$	E_T $[\hbar\omega_0]$
1	$\frac{1}{2}^+[660]$	0.95	0.315	24.205
2	$\frac{3}{2}^+[651]$	1.00	0.268	24.163
3	$\frac{3}{2}^-[521]$	1.04	0.230	24.126
4	$\frac{5}{2}^+[642]$	1.08	0.193	24.091
5	$\frac{5}{2}^-[523]$	1.11	0.166	24.065
6	$\frac{7}{2}^+[633]$	1.26	0.091	23.996
7	$\frac{1}{2}^-[521]$	1.28	0.117	24.010
8	$\frac{5}{2}^-[512]$	1.33	0.170	24.051
9	$\frac{7}{2}^-[514]$	1.42	0.258	24.132
10	$\frac{9}{2}^+[624]$	1.51	0.345	24.218
11	$\frac{1}{2}^-[510]$	1.52	0.355	24.227
12	$\frac{3}{2}^-[512]$	1.59	0.424	24.295

Legend: ε_ν = Nilsson single-particle energy,
E_ν = quasiparticle energy,
E_T = total energy of the nucleus.

Neglect of pair correlations leads to unreasonable matrix elements and serious disagreement with experimental results. Therefore the quasiparticle picture must be applied. BCS calculations have been performed with a set of 36 single-particle levels using $G_n = 0.021\ \hbar\omega_0 = 26.7/A$ MeV ($\hbar\omega_0 = 41\ A^{-\frac{1}{3}}$ MeV = 7.45 MeV). The energies near the Fermi level were taken from the energy set I reported in ref. [31]) with only the single-particle level $\frac{7}{2}^-[514]$ shifted by $-0.03\ \hbar\omega_0$. The other energies were adopted from ref. [32]). The single-particle states near the Fermi level are summarized in table 4. In column 3 the single-particle energies are listed and in columns 4 and 5 the quasiparticle energies

$$E_\nu = [(\varepsilon_\nu - \lambda - GV_\nu^2)^2 + \Delta_\nu^2]^{\frac{1}{2}}$$

and the total energy E_T of the odd nucleus are given. If ε_i is the single-particle energy of the blocked level, then

$$E_T = \varepsilon_i + 2\sum_{\nu \neq i} V_\nu^2(\varepsilon_\nu - \tfrac{1}{2}GV_\nu^2) - \Delta_i^2/G.$$

TABLE 5

Pairing factors for one-quasiparticle matrix elements $(U_k^{(i)}U_i^{(k)} - \beta V_k^{(i)}V_i^{(k)}) \prod_{\nu \neq i,\, k} (U_\nu^{(i)}U_\nu^{(k)} + V_\nu^{(i)}V_\nu^{(k)})$

	1	2	3	4	5	6	7	8	9	10	11	12
1		−0.94	−0.93	−0.92	−0.90	−0.54	−0.45	−0.26	−0.09	−0.003	0.003	0.04
2	0.99		−0.92	−0.91	−0.89	−0.52	−0.43	−0.23	−0.05	0.04	0.04	0.08
3	0.99	0.99		−0.90	−0.88	−0.50	−0.40	−0.19	−0.002	0.08	0.09	0.12
4	0.99	0.99	0.99		−0.86	−0.46	−0.35	−0.13	0.07	0.15	0.16	0.19
5	0.99	0.99	0.99	0.99		−0.42	−0.29	−0.06	0.14	0.22	0.23	0.26
6	0.69	0.71	0.72	0.75	0.78		0.73	0.78	0.80	0.81	0.81	0.81
7	0.65	0.66	0.69	0.72	0.75	0.99		0.81	0.84	0.85	0.85	0.86
8	0.52	0.54	0.57	0.61	0.65	0.96	0.99		0.90	0.91	0.91	0.91
9	0.39	0.42	0.45	0.50	0.56	0.92	0.96	0.99		0.94	0.95	0.95
10	0.33	0.36	0.40	0.45	0.51	0.90	0.94	0.98	0.99		0.96	0.97
11	0.32	0.36	0.39	0.45	0.51	0.89	0.94	0.98	0.99	1.00		0.97
12	0.30	0.33	0.37	0.43	0.49	0.88	0.93	0.97	0.99	1.00	1.00	

Upper triangle $\beta = +1$; lower triangle $\beta = -1$. The orbitals are numbered according to table 4.

TABLE 6

Theoretical structure of excited states in ^{167}Er

J^π	E_{exp} (keV)	E_{theor} (keV)	Components									
$\frac{7}{2}^+$	0	0	$\frac{7}{2}^+[633]$	90 %,	$\frac{7}{2}^+[633]+Q_{20}$	6 %,	$\frac{5}{2}^+[642]$	3 %				
$\frac{9}{2}^+$	79	54	$\frac{7}{2}^+[633]$	86 %,	$\frac{7}{2}^+[633]+Q_{20}$	6 %,	$\frac{5}{2}^+[642]$	6 %				
$\frac{1}{2}^-$	208	192	$\frac{1}{2}^-[521]$	92 %,	$\frac{1}{2}^-[521]+Q_{20}$	2 %,	$\frac{3}{2}^-[521]+Q_{2-2}$	3 %,	$\frac{5}{2}^-[523]+Q_{2-2}$	2 %		
$\frac{3}{2}^-$	265	248	$\frac{1}{2}^-[521]$	90 %,	$\frac{1}{2}^-[521]+Q_{20}$	2.5 %,	$\frac{3}{2}^-[521]+Q_{2-2}$	2 %,	$\frac{5}{2}^-[523]+Q_{2-2}$	2 %		
			$\frac{5}{2}^-[512]+Q_{2-2}$	1 %,	$\frac{1}{2}^-[510]$	1 %						
$\frac{5}{2}^-$	282	259	$\frac{1}{2}^-[521]$	92 %,	$\frac{1}{2}^-[521]+Q_{20}$	3 %,	$\frac{3}{2}^-[521]+Q_{2-2}$	2.5 %,	$\frac{5}{2}^-[523]+Q_{2-2}$	2 %		
$\frac{7}{2}^-$	413	388	$\frac{1}{2}^-[521]$	88 %,	$\frac{1}{2}^-[521]+Q_{20}$	3 %,	$\frac{3}{2}^-[521]+Q_{2-2}$	2 %,	$\frac{5}{2}^-[523]+Q_{2-2}$	1.5 %		
			$\frac{5}{2}^-[512]+Q_{2-2}$	2 %,	$\frac{1}{2}^-[510]$	2 %						
$\frac{9}{2}^-$	442	407	$\frac{1}{2}^-[521]$	90 %,	$\frac{1}{2}^-[521]+Q_{20}$	3.5 %,	$\frac{3}{2}^-[521]+Q_{2-2}$	2.5 %,	$\frac{5}{2}^-[523]+Q_{2-2}$	2 %		
$\frac{5}{2}^-$	347	392	$\frac{5}{2}^-[512]$	86 %,	$\frac{1}{2}^-[510]+Q_{22}$	11 %,	$\frac{1}{2}^-[521]+Q_{22}$	1 %				
$\frac{7}{2}^-$	430	479										
$\frac{9}{2}^-$	537	588	$\frac{5}{2}^-[512]$	84 %,	$\frac{1}{2}^-[510]+Q_{22}$	11 %,	$\frac{1}{2}^-[521]+Q_{22}$	1 %,	$\frac{3}{2}^-[521]$	2 %		
$\frac{5}{2}^-$	668	647	$\frac{5}{2}^-[523]$	81 %,	$\frac{1}{2}^-[521]+Q_{22}$	16 %,	$\frac{5}{2}^-[523]+Q_{20}$	2 %				
$\frac{7}{2}^-$	746	723	$\frac{5}{2}^-[523]$	80 %,	$\frac{1}{2}^-[521]+Q_{22}$	14 %,	$\frac{5}{2}^-[523]+Q_{20}$	2 %,	$\frac{5}{2}^-[512]$	1 %,	$\frac{7}{2}^-[514]$	1 %
$\frac{9}{2}^-$	845	823	$\frac{5}{2}^-[523]$	79 %,	$\frac{1}{2}^-[521]+Q_{22}$	12 %,	$\frac{5}{2}^-[523]+Q_{20}$	2 %,	$\frac{5}{2}^-[512]$	2 %,	$\frac{7}{2}^-[514]$	2.5 %
$\frac{5}{2}^+$	(592)	614	$\frac{5}{2}^+[642]$	79 %,	$\frac{5}{2}^+[642]+Q_{20}$	12 %,	$\frac{3}{2}^+[651]$	7.5 %,	$\frac{3}{2}^+[651]+Q_{20}$	1.5 %		
$\frac{7}{2}^+$	(654)	655	$\frac{5}{2}^+[642]$	69 %,	$\frac{5}{2}^+[642]+Q_{20}$	12 %,	$\frac{3}{2}^+[651]$	13 %,	$\frac{3}{2}^+[651]+Q_{20}$	2.5 %,	$\frac{7}{2}^+[633]$	3 %
$\frac{9}{2}^+$		717	$\frac{5}{2}^+[642]$	61 %,	$\frac{5}{2}^+[642]+Q_{20}$	11 %,	$\frac{3}{2}^+[651]$	17 %,	$\frac{3}{2}^+[651]+Q_{20}$	3.5 %,	$\frac{7}{2}^+[633]$	6 %
$\frac{3}{2}^-$	753	816	$\frac{1}{2}^-[521]+Q_{2-2}$	61 %,	$\frac{3}{2}^-[521]$	37 %						
$\frac{5}{2}^-$	810	881	$\frac{1}{2}^-[521]+Q_{2-2}$	60 %,	$\frac{3}{2}^-[521]$	36 %,	$\frac{5}{2}^-[512]+Q_{2-2}$	1 %				
$\frac{7}{2}^-$	896	978	$\frac{1}{2}^-[521]+Q_{2-2}$	54 %,	$\frac{3}{2}^-[521]$	36 %,	$\frac{5}{2}^-[512]+Q_{2-2}$	3.5 %,	$\frac{1}{2}^-[521]$	1 %,		
			$\frac{5}{2}^-[523]$	1.5 %,	$\frac{1}{2}^-[510]$	1.5 %						
$\frac{11}{2}^+$	711	835	$\frac{7}{2}^+[633]+Q_{22}$	94 %,	$\frac{5}{2}^+[642]+Q_{22}$	4.8 %						

$\frac{5}{2}^-$	852	800	$\frac{5}{2}^-[512]+Q_{2-2}$	55 %,	$\frac{1}{2}^-[510]$	37.5 %,	$\frac{3}{2}^-[512]+Q_{2-2}$	5 %,	$\frac{1}{2}^-[521]+Q_{2-2}$	2 %			
$\frac{7}{2}^-$	940	880	$\frac{5}{2}^-[512]+Q_{2-2}$	49 %,	$\frac{1}{2}^-[510]$	34 %,	$\frac{3}{2}^-[512]+Q_{2-2}$	5 %,	$\frac{1}{2}^-[521]+Q_{2-2}$	6 %,	$\frac{1}{2}^-[521]$	2 %	
			$\frac{3}{2}^-[521]+Q_{2-2}$	1 %									
$\frac{3}{2}^+$	532	757	$\frac{7}{2}^+[633]+Q_{2-2}$	81 %,	$\frac{3}{2}^+[651]$	15 %,	$\frac{3}{2}^+[651]+Q_{20}$	3 %					
$\frac{5}{2}^+$	574	803	$\frac{7}{2}^+[633]+Q_{2-2}$	84 %,	$\frac{3}{2}^+[651]$	10 %,	$\frac{3}{2}^+[651]+Q_{20}$	2 %,	$\frac{5}{2}^+[642]$	1 %,	$\frac{5}{2}^+[642]+Q_{2-2}$	2 %	
$\frac{7}{2}^+$		862	$\frac{7}{2}^+[633]+Q_{2-2}$	85 %,	$\frac{3}{2}^+[651]$	7 %,	$\frac{3}{2}^+[651]+Q_{22}$	1 %,	$\frac{3}{2}^+[624]+Q_{2-2}$	1 %,	$\frac{5}{2}^+[642]+Q_{2-2}$	5 %	
$\frac{5}{2}^-$	(1059)	1128	$\frac{1}{2}^-[521]+Q_{22}$	80 %,	$\frac{5}{2}^-[523]$	15 %,	$\frac{3}{2}^-[512]$	2 %					
$\frac{7}{2}^-$		1232	$\frac{1}{2}^-[521]+Q_{22}$	56 %,	$\frac{5}{2}^-[523]$	13 %,	$\frac{1}{2}^-[510]+Q_{2-2}$	2 %,	$\frac{7}{2}^-[514]$	18 %,			
			$\frac{7}{2}^-[514]+Q_{2-2}$	2.5 %,	$\frac{3}{2}^-[512]$	4 %,	$\frac{3}{2}^-[512]+Q_{22}$	1.5 %					
$\frac{3}{2}^-$	1086	1409	$\frac{3}{2}^-[521]$	60 %,	$\frac{1}{2}^-[521]+Q_{2-2}$	37 %,	$\frac{3}{2}^-[521]+Q_{20}$	2 %					
$\frac{5}{2}^-$	1135	1474	$\frac{3}{2}^-[521]$	58 %,	$\frac{1}{2}^-[521]+Q_{2-2}$	36 %,	$\frac{3}{2}^-[521]+Q_{20}$	2 %,	$\frac{5}{2}^-[523]+Q_{2-2}$	2 %			
$\frac{7}{2}^-$	1206	1567	$\frac{3}{2}^-[521]$	55 %,	$\frac{1}{2}^-[521]+Q_{2-2}$	36 %,	$\frac{3}{2}^-[521]+Q_{20}$	3 %,	$\frac{5}{2}^-[523]+Q_{2-2}$	2.5 %,	$\frac{5}{2}^-[512]+Q_{2-2}$	1 %	
$\frac{7}{2}^-$		1112	$\frac{7}{2}^-[514]$	68 %,	$\frac{3}{2}^-[512]+Q_{22}$	9 %,	$\frac{1}{2}^-[521]+Q_{22}$	21 %,					
$\frac{9}{2}^-$		1212	$\frac{7}{2}^-[514]$	56 %,	$\frac{3}{2}^-[512]+Q_{22}$	8 %,	$\frac{1}{2}^-[521]+Q_{22}$	31 %,	$\frac{3}{2}^-[521]$	1 %			
$\frac{3}{2}^-$	1384	1295	$\frac{3}{2}^-[512]$	41 %,	$\frac{7}{2}^-[514]+Q_{2-2}$	38 %,	$\frac{1}{2}^-[510]+Q_{2-2}$	16 %,	$\frac{5}{2}^-[523]+Q_{2-2}$	3 %			
$\frac{5}{2}^-$	1444	1360	$\frac{3}{2}^-[512]$	37 %,	$\frac{7}{2}^-[514]+Q_{2-2}$	36 %,	$\frac{1}{2}^-[510]+Q_{2-2}$	14 %,	$\frac{5}{2}^-[523]+Q_{2-2}$	8 %,			
			$\frac{1}{2}^-[521]+Q_{22}$	2 %,	$\frac{3}{2}^-[521]$	1 %,							
$\frac{7}{2}^-$	1526	1454	$\frac{3}{2}^-[512]$	32 %,	$\frac{7}{2}^-[514]+Q_{2-2}$	33 %,	$\frac{1}{2}^-[510]+Q_{2-2}$	11 %,	$\frac{5}{2}^-[523]+Q_{2-2}$	15 %,			
			$\frac{1}{2}^-[521]+Q_{22}$	5 %,	$\frac{3}{2}^-[521]$	2 %,							
$\frac{1}{2}^-$		1462	$\frac{5}{2}^-[523]+Q_{2-2}$	97 %,	$\frac{1}{2}^-[521]+Q_{20}$	2 %,	$\frac{1}{2}^-[521]$	1 %					
$\frac{3}{2}^-$		1504	$\frac{5}{2}^-[523]+Q_{2-2}$	92 %,	$\frac{1}{2}^-[521]+Q_{20}$	1 %,	$\frac{1}{2}^-[521]$	1 %,	$\frac{3}{2}^-[521]+Q_{2-2}$	2 %,	$\frac{3}{2}^-[512]$	2 %	
$\frac{5}{2}^-$		1588	$\frac{5}{2}^-[523]+Q_{2-2}$	85 %,	$\frac{1}{2}^-[521]+Q_{20}$	4 %,	$\frac{1}{2}^-[521]$	1 %,	$\frac{7}{2}^-[514]+Q_{2-2}$	2 %,	$\frac{3}{2}^-[512]$	4 %,	
			$\frac{1}{2}^-[510]+Q_{2-2}$	2 %									
$\frac{1}{2}^-$	(1179)	1720	$\frac{1}{2}^-[521]+Q_{20}$	93 %,	$\frac{1}{2}^-[521]$	2 %,	$\frac{5}{2}^-[523]+Q_{2-2}$	1 %,	$\frac{3}{2}^-[521]+Q_{2-2}$	4 %			
$\frac{3}{2}^-$	(1227)	1791	$\frac{1}{2}^-[521]+Q_{20}$	90 %,	$\frac{1}{2}^-[521]$	2 %,	$\frac{5}{2}^-[512]+Q_{2-2}$	1 %,	$\frac{3}{2}^-[521]+Q_{2-2}$	7 %			
$\frac{5}{2}^-$	(1254)	1811	$\frac{1}{2}^-[521]+Q_{20}$	90 %,	$\frac{1}{2}^-[521]$	2 %,	$\frac{5}{2}^-[523]+Q_{2-2}$	3 %,	$\frac{3}{2}^-[521]+Q_{2-2}$	4 %			
$\frac{7}{2}^-$		1972	$\frac{1}{2}^-[521]+Q_{20}$	81 %,	$\frac{1}{2}^-[521]$	1 %,	$\frac{5}{2}^-[512]+Q_{2-2}$	2 %,	$\frac{3}{2}^-[521]+Q_{2-2}$	12 %,	$\frac{1}{2}^-[510]$	1 %	
$\frac{1}{2}^-$		1970	$\frac{3}{2}^-[521]+Q_{2-2}$	93 %,	$\frac{1}{2}^-[521]$	4 %,	$\frac{1}{2}^-[521]+Q_{20}$	3 %					

The relative energies of the one-quasiparticle states may be taken either from the differences of the E_ν, as has been done in this calculation, or alternatively from the differences of the corresponding E_T values. The results of both methods are nearly the same for states far away from the Fermi level, whereas for states near the Fermi level the excitation energies calculated from the E_T are somewhat smaller than those derived from the E_ν. The blocking effect has been taken into account in the way described in ref. [1]).

In table 5 the factors are given by which the single-particle matrix elements are reduced as a consequence of pairing correlations. The factors in the upper triangle apply to matrix elements of operators which commute with the time-reversal operator, as do the $E\lambda$ multipole operators and the operators of the quasiparticle-phonon interaction. The reduction factors corresponding to matrix elements of operators which anticommute with the time-reversal operator such as the Coriolis coupling are listed in the lower triangle. As can be seen from the table, the pairing factors may deviate considerably from unity. This explains the discrepancies which are obtained, when pairing correlations are not taken into account.

Diagonalization has been performed using the orbitals summarized in table 4 together with the connected beta- and gamma-vibrational states (cf. ref. [1])). The Nilsson functions were calculated with $\mu = 0.45$, $\kappa = 0.05$ and $\delta = 0.3$. It turned out that inclusion of the orbital $\frac{1}{2}^+[660]$ requires the introduction of additional parameters since this state causes unreasonable distortion of the positive parity bands. In order to avoid the use of additional parameters the results reported here come from calculations which do not include the orbital $\frac{1}{2}^+[660]$.

The calculations are based on the following parameters: $\varepsilon = \hbar/J_0 = 22$ keV, $E_\gamma = 685$ keV, $E_\beta = 1350$ keV. Here, ε is the rotational parameter with the undisturbed moment of inertia J_0 and E_γ and E_β are the gamma and beta vibrational energies. While ε was fitted, E_γ and E_β were deduced from the level scheme of the neighbouring nucleus ^{166}Er by applying a proper correction for the blocking effect.

The gamma-vibrational band in ^{166}Er is well established to occur at 786 keV. As concerns the beta vibration, the situation is still unsettled. A 0^+ state has been identified in the decay [33]) of ^{166}Ho at 1460 keV excitation energy. However, in a study of the inelastic scattering of deuterons [34]) this level was not observed and the authors therefore conclude that it is hardly connected with a collective beta vibration. On the other hand, no alternative level could be detected in the (d, d′) reaction as belonging to a $K = 0$ band below 2500 keV and for the other even erbium isotopes the cross sections for exciting the beta vibration were in general found to be small. Thus the level observed in the ^{166}Ho decay provides the only indication of a 0^+ state in ^{166}Er. It is worth mentioning that we could very recently † identify the first $K = 0$ band in ^{168}Er at 1215 keV with rotational levels at 1277 keV (2^+) and 1411 keV (4^+). Theoretical considerations within the quasi-boson approximation [35]) predict very similar beta vibrational energies for ^{166}Er and ^{168}Er. Fortunately

† See preliminary decay scheme in fig. 7, ref. [16]). Details given in ref. [13]).

the results of the present calculations are rather insensitive to the choice of E_β except for the excitation energy of the beta bands themselves.

Table 6 summarizes the theoretical energies and structures of individual levels in ^{167}Er as obtained from the described model.

6. Comparison of experimental and theoretical results

6.1. EXCITATION ENERGIES

In fig. 3 the calculated excitation energies for ^{167}Er are compared with the experimental level scheme. In general, the agreement is surprisingly good and this result supports the spectroscopic interpretation of the observed rotational bands.

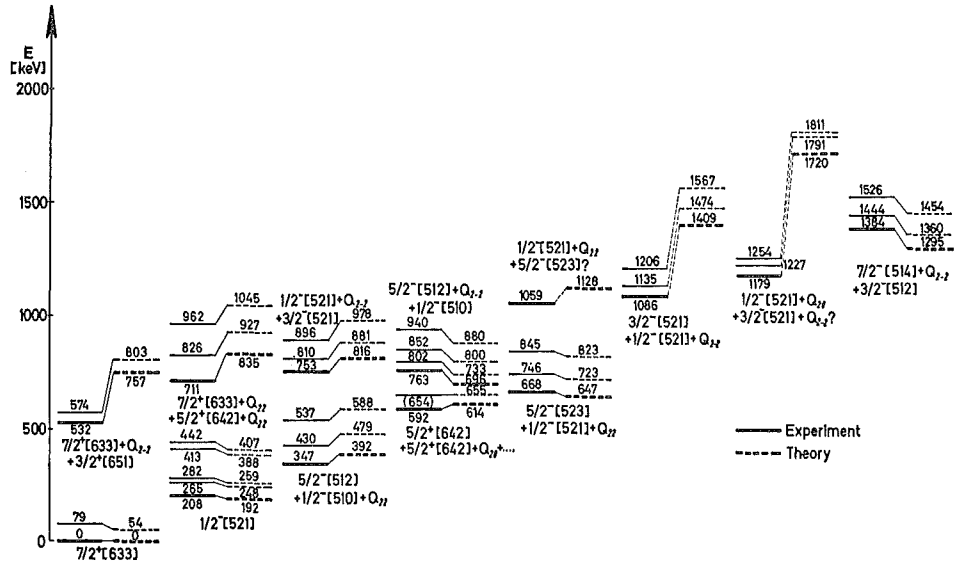

Fig. 3. Comparison of experimental and theoretical excitation energies in ^{167}Er.

Not only the bandhead energies, but also the moments of inertia and the decoupling parameters are predicted quite well. It is not unexpected that the correspondence of the data becomes worse above 1 MeV excitation energy. In this region the structure of the levels is much more complicated than it can result from the present model. In particular, the neglect of octupole vibrations and noncollective three-quasiparticle configurations affects the theory at higher energies increasingly. With respect to the band $\frac{1}{2}^-[521]+Q_{20}+\ldots$, the uncertainty in E_β as derived from ^{166}Er directly enters into the result (cf. sect. 5).

6.2. TRANSITION PROBABILITIES AND MULTIPOLE MIXTURES

The occurrence of strong band mixing is responsible for various phenomena which cannot be explained within the framework of simple models. For illustration, tran-

TABLE 7

Transition probabilities and multipole mixtures

E_i (keV)	Level $\mathcal{J}_i\pi_i K_i$	Transition 1 $\mathcal{J}_f\pi_f K_f$	Transition 1 multipolarity	Transition 2 $\mathcal{J}_{f'}\pi_{f'} K_{f'}$	Transition 2 multipolarity	δ^2_{theor} $H' \neq 0$	δ'^2_{theor} $H' \neq 0$	Intensity ratio I/I' Theory [a]) $H' = 0$	Theory [a]) $H' \neq 0$	Experiment
532	$\frac{3}{2}^+ \frac{3}{2}$	$\frac{1}{2}^- \frac{1}{2}$	E1	$\frac{7}{2}^+ \frac{7}{2}$	E2			0	0.0043	0.0013 ±0.0003 [b])
		$\frac{3}{2}^- \frac{1}{2}$	E1	$\frac{7}{2}^+ \frac{7}{2}$	E2			0	0.0032	0.0014 ±0.0003 [b])
		$\frac{5}{2}^- \frac{1}{2}$	E1	$\frac{7}{2}^+ \frac{7}{2}$	E2			0	0.0001	0.0014 ±0.0003 [b])
668	$\frac{5}{2}^- \frac{5}{2}$	$\frac{3}{2}^- \frac{1}{2}$	M1+E2	$\frac{1}{2}^- \frac{1}{2}$	E2	8.6		0.59 [c])	0.76	1.57 ±0.25 [b])
		$\frac{5}{2}^- \frac{1}{2}$	M1+E2	$\frac{1}{2}^- \frac{1}{2}$	E2	7.9		0.27 [c])	1.04	1.62 ±0.26 [b])
		$\frac{3}{2}^- \frac{1}{2}$	M1+E2	$\frac{5}{2}^- \frac{5}{2}$	M1+E2	8.6	≈0	0.0014 [d])	0.82	0.14 ±0.01 [b])
										0.21 ±0.07 [c])
753	$\frac{3}{2}^- \frac{3}{2}$	$\frac{3}{2}^- \frac{1}{2}$	M1+E2	$\frac{1}{2}^- \frac{1}{2}$	M1+E2	0.48	0.13	0.57	0.45	0.77 $^{+0.33}_{-0.19}$
		$\frac{5}{2}^- \frac{1}{2}$	M1+E2	$\frac{1}{2}^- \frac{1}{2}$	M1+E2	0.82	0.13	0.21	0.11	≈ 0.13
763	$\frac{1}{2}^- \frac{1}{2}$	$\frac{3}{2}^- \frac{1}{2}$	M1+E2	$\frac{5}{2}^- \frac{5}{2}$	E2	0.02		0	6.2	4.1 $^{+1.1}_{-0.8}$
		$\frac{3}{2}^- \frac{1}{2}$	M1+E2	$\frac{1}{2}^- \frac{1}{2}$	M1	0.02	0	[f])	1570	≳ 15
802	$\frac{3}{2}^- \frac{1}{2}$	$\frac{1}{2}^- \frac{1}{2}$	M1+E2	$\frac{5}{2}^- \frac{5}{2}$	M1+E2	0.18	24	0	6.4	10.0 $^{+5.5}_{-3.0}$
		$\frac{5}{2}^- \frac{1}{2}$	M1+E2	$\frac{1}{2}^- \frac{1}{2}$	M1+E2	0.17	0.18	[f])	0.19	0.15 $^{+0.7}_{-0.6}$
1059	$\frac{5}{2}^- \frac{5}{2}$	$\frac{1}{2}^- \frac{1}{2}$	E2	$\frac{3}{2}^- \frac{1}{2}$	M1+E2		83	1.24	1.09	< 4 [g])
		$\frac{5}{2}^- \frac{1}{2}$	M1+E2	$\frac{3}{2}^- \frac{1}{2}$	M1+E2	28	83	0.50	0.40	0.39 $^{+0.23}_{-0.17}$
		$\frac{7}{2}^- \frac{1}{2}$	M1+E2	$\frac{3}{2}^- \frac{1}{2}$	M1+E2	26	83	0.12	0.24	≈ 2 [h])
1086	$\frac{3}{2}^- \frac{3}{2}$	$\frac{3}{2}^- \frac{1}{2}$	M1+E2	$\frac{1}{2}^- \frac{1}{2}$	M1+E2	0.13	0.13	0.65	0.70	[i])
		$\frac{5}{2}^- \frac{1}{2}$	M1+E2	$\frac{1}{2}^- \frac{1}{2}$	M1+E2	0.33	0.13	0.15	0.18	< 0.3
1206	$\frac{7}{2}^- \frac{3}{2}$	$\frac{5}{2}^- \frac{1}{2}$	M1+E2	$\frac{3}{2}^- \frac{1}{2}$	E2	0.08		10^{-3}	20	≈ 2
1179	$\frac{1}{2}^- \frac{1}{2}$	$\frac{1}{2}^- \frac{1}{2}$	M1	$\frac{3}{2}^- \frac{1}{2}$	M1+E2		$5 \cdot 10^3$	0	10^{-3}	> 0.3
1227	$\frac{3}{2}^- \frac{1}{2}$	$\frac{3}{2}^- \frac{1}{2}$	M1+E2	$\frac{1}{2}^- \frac{1}{2}$	M1+E2	100	10^4	0.75	0.82	0.44 $^{+0.19}_{-0.12}$

[a]) Here, $H' = 0$ refers to the adiabatic model including pair correlations; $H' \neq 0$ gives the results when all interaction terms are taken into account.
[b]) Intensities taken from ref. [7]).
[c]) Both transitions have multipolarity E2. M1 transitions are K-forbidden.
[d]) Transition 1 is pure E2 radiation, M1 is K-forbidden.
[e]) Derived from table 2.
[f]) In the adiabatic model both transitions do not exist.
[g]) Transition 1 obscured.
[h]) See text (sect. 4).
[i]) Transition 1 obscured by a strong gamma ray from ^{168}Er.

sition probabilities and multipole mixtures have been calculated for several transitions assuming both $H' = 0$ and $H' \neq 0$. In table 7 the results are compared with the experimental data. In the adiabatic case the levels were identified with the dominant component from table 6. This is in reasonable correspondence with the Nilsson model and the beta- and gamma-vibrational energies.

The transition rates have been calculated using [36,37]) $g_R = 0.18$, $g_l = 0$, $(g_s)_{eff} = f(-3.83)$ with $f = 0.6$ and $e_{eff} = 1.0\,e$. For determining the E2 transition probabilities quadratic terms have been included in the collective part of the E2 operator [1]).

Several one-quasiparticle states, in particular the orbital $\frac{3}{2}^+[651]$, are admixed into the gamma vibrational band at 532 keV. These admixtures give rise to the presence of some single-particle strength in the (d, p) reaction and to the occurrence of E1 transitions to the orbital $\frac{1}{2}^-[521]$. With $H' \neq 0$ the intensity of these transitions is predicted in the correct order of magnitude †.

As a consequence of band mixing the E2 radiation connecting the orbitals $\frac{5}{2}^-[523]$ and $\frac{1}{2}^-[521]$ is enhanced and the transitions contain small admixtures of M1 radiation. A consequence of mixing between the configurations $\frac{1}{2}^-[521]+Q_{2-2}$ and $\frac{3}{2}^-[521]$ is that both rotational bands are de-excited to the $\frac{1}{2}^-$ [521] band predominantly by M1 transitions.

A very obvious example for strong configuration mixing is provided by the $\frac{1}{2}^-$ rotational band observed at 763 keV. The only Nilsson state with spin and parity $\frac{1}{2}^-$ near the Fermi level is the orbital $\frac{1}{2}^-[521]$. This state, however, is well established to occur at 208 keV excitation energy. In addition, the assumption of a pure Nilsson band requires that the intensity ratio for the gamma rays proceeding from the bandhead to the $\frac{3}{2}^-$ and $\frac{1}{2}^-$ levels at 265 and 208 keV is 7.0 which is in disagreement with the experimental value $\gtrapprox 15$. Thus it is reasonable to assume that the band at 763 keV corresponds to the gamma vibrational band based upon the configuration $\frac{5}{2}^-[512]$ and, in fact, a collective E2 transition leaving the bandhead is observed. In other respects, however, the de-excitation shows clear anomalies. From both the first and second member of the band transitions proceed to the $\frac{1}{2}^-[521]$ Nilsson state which in intensity considerably surpass the E2 transitions to the "own" intrinsic configuration. Furthermore, the branching ratio to the $\frac{3}{2}^-$ and $\frac{1}{2}^-$ levels is exceptional. A reasonable explanation for these anomalies is provided by assuming a strong admixture of the $\frac{1}{2}^-$ [510] Nilsson state in the $\frac{5}{2}^-[512]+Q_{2-2}$ excitation. It is true that the $\frac{1}{2}^-[510]$ orbital is expected at much higher energies, but it is connected with the $\frac{5}{2}^-[512]$ state by a strong E2 matrix element. In sect. 5 the admixture was calculated to be 38 %. On the other hand, the rotational band at 208 keV consists only to 92 % of the Nilsson state $\frac{1}{2}^-[521]$. As can be seen from table 7, the band mixing resulting from H' explains the observed anomalies quite well. Obviously, the transition to the $\frac{3}{2}^-$ level is strongly enhanced compared to that reaching the $\frac{1}{2}^-$ state and, in fact, in none

† After completion of the manuscript we got knowledge of a study in which the rotation-vibration interaction between the ground state and the associated $K\pm2$ gamma vibrational bands is investigated by means of Coulomb excitation with ^{16}O ions [38]).

of the hitherto known investigations of the nuclei ^{165}Dy, ^{167}Er and ^{169}Yb a transition to the $\frac{1}{2}^-$ level has been detected.

Provided that the interpretation of the 1179 keV band as a beta vibration is correct, then the intensity of the 971 keV M1 transition represents a sensitive criterion for the strength of single-particle admixtures. Presumably the structure is however more complicated than predicted by the present model (cf. subsect. 6.1) and this might explain the still insufficient agreement between theory and experiment for the transitions leaving the state at 1179 keV.

When judging the theoretical branching ratios in table 7, one should notice that we are not dealing with a simple procedure such as that applied in the Alaga rule, but that the nuclear wave functions of three states directly enter into the result.

Till now there are no internal conversion data available on ^{167}Er from neutron capture. It would be very interesting to check the theoretical predictions on the multipole mixtures by such measurements.

6.3. PARTIAL GAMMA-RAY HALF-LIVES

In general, the low-lying excited states are expected to be essentially characterized by pure wave functions and, in fact, only small admixtures are predicted for these states by the calculations described above. Nevertheless even small admixtures may have a decisive influence on the partial gamma-ray half-lives. This is demonstrated in table 8 where the theoretical values both for $H' = 0$ and $H' \neq 0$ are compared with

TABLE 8

Partial gamma-ray half-lives $T_{\frac{1}{2}\gamma}$

Nucleus	Initial configuration	Final configuration	Multipolarity	δ^2_{theor}	$T_{\frac{1}{2}\gamma}$(nsec)		
					$H' = 0$	$H' \neq 0$	exp.
^{167}Er	$\frac{1}{2}^-$ $\frac{1}{2}$[521]	$\frac{7}{2}^+$ $\frac{7}{2}$[633]	E3		3.6 sec	4.3 sec	5.5 sec [a]
	$\frac{3}{2}^-$ $\frac{1}{2}$[521]	$\frac{1}{2}^-$ $\frac{1}{2}$[521]	M1+E2	0.74	13.5	23.5	39.4 [b]
	$\frac{5}{2}^-$ $\frac{5}{2}$[512]	$\frac{7}{2}^+$ $\frac{7}{2}$[633]	E1		0.07	0.1	1.0 [c]
		$\frac{1}{2}^-$ $\frac{1}{2}$[521]	E2	∞	$8.3 \cdot 10^4$	517	
		$\frac{3}{2}^-$ $\frac{1}{2}$[521]	M1+E2	0.030	$1.0 \cdot 10^6$	85	
		$\frac{5}{2}^-$ $\frac{1}{2}$[521]	M1+E2	0.003	$5.7 \cdot 10^6$	99	
	$\frac{3}{2}^+$ ($\frac{7}{2}$[633]+Q_{2-2})	$\frac{7}{2}^+$ $\frac{7}{2}$[633]	E2	∞	$7.7 \cdot 10^{-3}$	$8.1 \cdot 10^{-3}$	$15 \cdot 10^{-3}$ [d]
^{169}Yb	$\frac{5}{2}^-$ $\frac{5}{2}$[512]	$\frac{7}{2}^+$ $\frac{7}{2}$[633]	E1		0.1	0.3	1.3 [b] 4.2 [a]
		$\frac{1}{2}^-$ $\frac{1}{2}$[521]	E2	∞	$2.1 \cdot 10^4$	630	102 [b] 320 [a]
		$\frac{3}{2}^-$ $\frac{1}{2}$[521]	M1+E2	0.055	$1.9 \cdot 10^5$	135	103 [b] 260 [a]
		$\frac{5}{2}^-$ $\frac{1}{2}$[521]	M1+E2	0.009	$6.3 \cdot 10^5$	110	84 [b] 220 [a]

[a]) Ref. [39]). [b]) Ref. [40]). [c]) Ref. [7]). [d]) Ref. [41]).

experimental data. In all cases the inclusion of band mixing yields an improvement of the theoretical predictions. This is particularly conspicuous for K-forbidden M1 transitions. Unfortunately the very weak gamma rays which de-excite the state $\frac{5}{2}^-[512]$ to the first three rotational members of the band $\frac{1}{2}^-[521]$ have not yet been observed for ^{167}Er. Therefore some data on ^{169}Yb have been included in the table for comparison. It would be very useful to identify the corresponding transitions in ^{167}Er and to measure their intensity, since they provide a direct check of the band mixing in the low-lying states. The gamma-ray energies are expected to be 65 keV, 82 keV and 139 keV. Thus a diffraction spectrometer will be the most promising instrument. A very high enrichment of the sample would be desirable.

7. Conclusions

Considerable band mixing effects occur in ^{167}Er. Experimentally these phenomena can thoroughly be studied by means of the radiative neutron capture process. A better understanding can be obtained within the framework of the unified model, if the interaction between all possible modes of nuclear motion is taken into account. The inclusion of pair correlations is essential for achieving agreement with experimental data. Various properties of the de-excitation mechanism are determined to a large extent by band mixing, even for low-lying states where the admixtures are small.

References

1) W. Michaelis, F. Weller, H. Schmidt, G. Markus and U. Fanger, Nucl. Phys. **A119** (1968) 609
2) G. Markus, W. Michaelis, H. Schmidt and C. Weitkamp, Z. Phys. **206** (1967) 84
3) H. R. Koch, Z. Phys. **187** (1965) 450
4) W. V. Prestwich and R. E. Coté, Phys. Rev. **162** (1967) 1112
5) R. A. Harlan and R. K. Sheline, Phys. Rev. **168** (1968) 1373
6) M. Rozkos, F. Sterba, J. Sterbova, B. Elbek and P. O. Tjøm, Int. Symp. on nuclear structure (Dubna, USSR, July 1968)
7) L. Funke, W. Andrejtscheff, H. Graber, U. Hagemann, K.-H. Kaun, P. Kemnitz, W. Meiling, H. Sodan, F. Stary and G. Winter, Nucl. Phys. **A118** (1968) 97
8) R. R. Chasman, Nucl. Phys. **89** (1966) 11
9) D. R. Bès and Cho Yi-Chung, Nucl. Phys. **86** (1966) 581
10) V. G. Soloviev, P. Vogel and G. Jungklausen, Rep. JINR E4-3051 (1966)
11) F. Weller, to be published; Int. Conf. on properties of nuclear states (Montreal, 1969)
12) Neutron cross sections, BNL-325, 2nd Ed., Suppl. 2, August 1966
13) W. Michaelis, H. Ottmar and F. Weller, to be published
14) W. Michaelis and H. Küpfer, Nucl. Instr. **56** (1967) 181
15) F. Horsch, O. Meyer and W. Michaelis, Proc. Int. Symp. on nuclear electronics (Versailles, 1968); KFK 778 (1968)
16) W. Michaelis and F. Horsch, Proc. Int. Symp. on neutron capture gamma-ray spectroscopy (Studsvik, 1969) ed. by IAEA, Vienna
17) U. Fanger, KFK 887 (1969)
18) G. Krüger, G. Dimmler, G. Zipf, H. Hanak and R. Merkel, Kerntechnik **8** (1966) 273
19) J. Legrand, J. P. Boulanger and J. P. Brethon, Nucl. Phys. **A107** (1968) 177
20) G. Murray, R. L. Graham and J. S. Geiger, Nucl. Phys. **63** (1965) 353
21) W. W. Black and R. L. Heath, Nucl. Phys. **90** (1967) 650

22) R. C. Greenwood and W. W. Black, Phys. Lett. **21** (1966) 702
23) J. B. Marion, Nucl. Data **A4** (1968) 316
24) G. E. Thomas, D. E. Batchley and L. M. Bollinger, Nucl. Instr. **56** (1967) 325
25) N. V. de Castro Faria and R. J. A. Lévesque, Nucl. Instr. **46** (1967) 325
26) D. G. Burke, B. Zeidman, B. Elbek, B. Herskind and M. Olesen, Mat. Fys. Medd. Dan. Vid. Selsk. **35**, No. 2 (1966)
27) V. Bondarenko, P. Prokofyev, P. Manfrass and A. Andreeff, Izv. Akad. Nauk Latv. SSR, No. 1 (1969) 3
28) A. Faessler, Nucl. Phys. **59** (1964) 177
29) A. Faessler, Nucl. Phys. **85** (1966) 679
30) S. G. Nilsson, Mat. Fys. Medd. Dan. Vid. Selsk. **29**, No. 16 (1955)
31) C. J. Gallagher, Jr. and V. G. Soloviev, Mat. Fys. Skr. Dan. Vid. Selsk. **2**, No. 2 (1962)
32) V. G. Soloviev, Atom. Energ. Rev. 3 (1965) 117
33) C. M. Lederer, J. M. Hollander and I. Perlman, Table of isotopes, 6th ed. (J. Wiley and Sons, Inc., New York, 1967)
34) P. O. Tjøm and B. Elbek, Nucl. Phys. **A107** (1968) 385
35) D. R. Bès, Nucl. Phys. **49** (1963) 544
36) Z. Bochnacki and S. Ogaza, Nucl. Phys. **69** (1965) 186
37) O. Prior, F. Boehm and S. G. Nilsson, Nucl. Phys. **A110** (1968) 257
38) A. Tveter and B. Herskind, Nucl. Phys. **A134** (1969) 599
39) K. E. G. Löbner and S. G. Malmskog, Nucl. Phys. **80** (1966) 505
40) H. Nabielek, SGAE PH-78/1968
41) Nucl. Data Sheets (1964)